Molecular Therapy
Original Article

Prevention of Photoreceptor Cell Loss in a *Cln6*^{nclf} Mouse Model of Batten Disease Requires *CLN6* Gene Transfer to Bipolar Cells

Sophia-Martha kleine Holthaus,[1,2] Joana Ribeiro,[1] Laura Abelleira-Hervas,[1] Rachael A. Pearson,[1] Yanai Duran,[1] Anastasios Georgiadis,[1] Robert D. Sampson,[1] Matteo Rizzi,[1] Justin Hoke,[1] Ryea Maswood,[1] Selina Azam,[1] Ulrich F.O. Luhmann,[1,7] Alexander J. Smith,[1] Sara E. Mole,[2,3,4,6] and Robin R. Ali[1,5,6]

[1]Department of Genetics, UCL Institute of Ophthalmology, 11-43 Bath Street, London EC1V 9EL, UK; [2]MRC Laboratory for Molecular Cell Biology, University College London, Gower Street, London WC1E 6BT, UK; [3]UCL Institute of Child Health, 30 Guilford Street, London WC1N 1EH, UK; [4]UCL Department of Genetics, Evolution and Environment, University College London, Gower Street, London WC1E 6BT, UK; [5]NIHR Biomedical Research Centre at Moorfields Eye Hospital NHS Foundation Trust and UCL Institute of Ophthalmology, City Road, London EC1V 2PD, UK

The neuronal ceroid lipofuscinoses (NCLs) are inherited lysosomal storage disorders characterized by general neurodegeneration and premature death. Sight loss is also a major symptom in NCLs, severely affecting the quality of life of patients, but it is not targeted effectively by brain-directed therapies. Here we set out to explore the therapeutic potential of an ocular gene therapy to treat sight loss in NCL due to a deficiency in the transmembrane protein CLN6. We found that, although *Cln6*^{nclf} mice presented mainly with photoreceptor degeneration, supplementation of CLN6 in photoreceptors was not beneficial. Because the level of *CLN6* is low in photoreceptors but high in bipolar cells (retinal interneurons that are only lost in *Cln6*-deficient mice at late disease stages), we explored the therapeutic effects of delivering *CLN6* to bipolar cells using adeno-associated virus (AAV) serotype 7m8. Bipolar cell-specific expression of *CLN6* slowed significantly the loss of photoreceptor function and photoreceptor cells. This study shows that the deficiency of a gene normally expressed in bipolar cells can cause the loss of photoreceptors and that this can be prevented by bipolar cell-directed treatment.

INTRODUCTION

The neuronal ceroid lipofuscinoses (NCLs) are rare, inherited lysosomal storage disorders that present with severe neurodegeneration and sight loss. This group of diseases is more commonly referred to as Batten disease, and at least 13 genes have been linked to the development of this condition with a combined incidence in different countries of between 1:12,500 and 1:100,000.[1] The affected genes code either for a soluble lysosomal protein or a transmembrane protein.[2] The development of therapies for forms of NCL caused by defects in lysosomal enzymes is aided by lysosomal cross-correction, which allows the therapeutic enzyme to be taken up by cells from the circulation and other cells via the mannose-6-phosphate pathway.[3] This phenomenon has helped to pave the way toward clinical trials for CLN2 disease, a common form of NCL arising from the deficiency in the lysosomal enzyme TPP1 (Clinical Trials.gov: NCT01907087). Cross-correction, however, does not occur for transmembrane proteins, limiting functional restoration to individual cells and increasing the challenge to achieve a therapeutic effect.

CLN3 disease with juvenile onset is the most common form of NCL that is caused by a defect in a membrane-bound protein.[4] Other rarer forms caused by transmembrane protein deficiencies include CLN6, CLN7, and CLN8 disease, all variant forms with typically a late-infantile onset and a more rapid progression than CLN3 disease. NCLs usually manifest with seizures, visual decline resulting in blindness, and progressive psychomotor and cognitive deteriorations. The order of the symptoms varies, yet these conditions collectively lead to premature death.[5] A major obstacle to developing brain-directed therapies for NCLs arising from transmembrane protein defects is the challenge to deliver agents throughout the brain. Recently, the partial rescue of the brain phenotype in a CLN3 disease mouse model was described following brain-directed adeno-associated virus (AAV)-mediated gene therapies.[6,7] No correction of the disease pathology was reported outside of the brain, underlining the need for treatments not only targeting the brain but also other affected organs like the eye. Moreover, ocular therapies may not only increase the quality of life of

Received 27 November 2017; accepted 27 February 2018;
https://doi.org/10.1016/j.ymthe.2018.02.027.

[6]These authors equally contributed to this work.

[7]Present address: Roche Pharmaceutical Research and Early Development, Translational Medicine Neuroscience & Biomarkers, Roche Innovation Center, Basel, Switzerland

Correspondence: Sara E. Mole, University College London, Gower Street, London WC1E 6BT, UK.
E-mail: s.mole@ucl.ac.uk
Correspondence: Robin R. Ali, University College London, Institute of Ophthalmology, Department of Genetics, 11-43 Bath Street, London EC1V 9EL, UK.
E-mail: r.ali@ucl.ac.uk

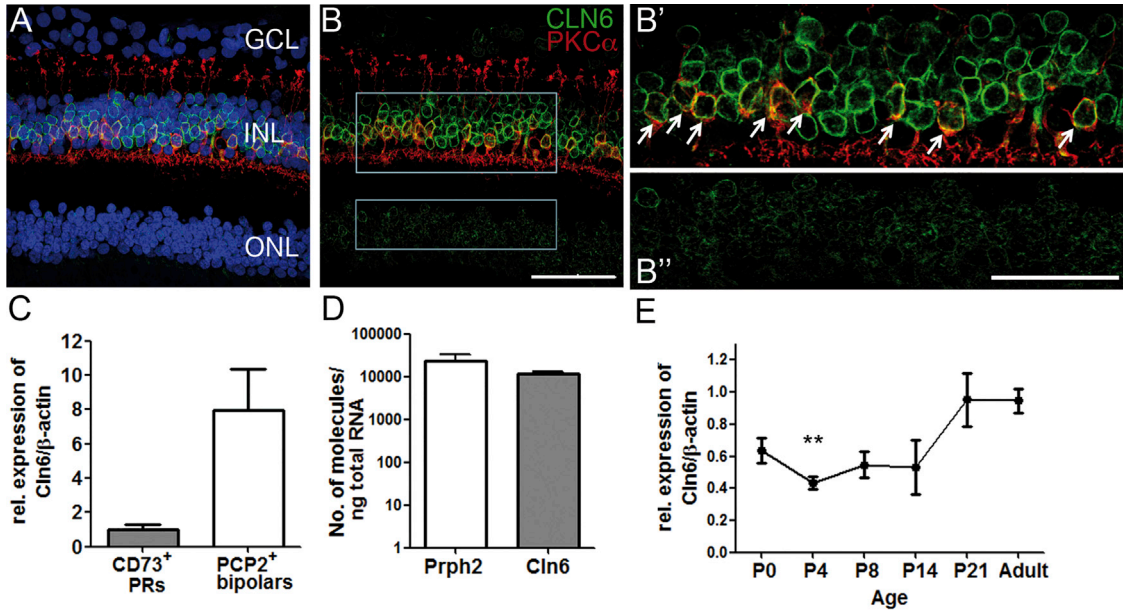

Figure 1. *CLN6* Is More Highly Expressed in Bipolar Cells Than in Photoreceptors in Human and Mouse Retina

Staining for CLN6 (green) and PKCα (red) on human retinal section showing high levels of CLN6 in the INL and lower levels in the ONL with (A) and without (B) DAPI nuclear counterstaining in blue. Gray boxes show areas of higher-magnification images. Scale bar, 50 μm. Single confocal image reveals (B') $CLN6^+$ rod bipolar cells (arrows) and (B") $CLN6^+$ cells in the ONL. Scale bar, 25 μm. (C) *Cln6* expression level in adult mouse bipolar cells relative to photoreceptors after normalization for β-actin (mean ± SEM; n = 3 samples of 3–5 pooled retinas each; not significant, Mann-Whitney U test). (D) Absolute expression levels of *Cln6* and *Peripherin2* in adult wild-type mouse retinas (means ± SEM). *Peripherin2*, n = 3 mice; $Cln6^{nclf}$, n = 4 mice. (E) Time course of the expression level of *Cln6* in wild-type mouse retinas relative to adult levels, normalized for β-actin (mean ± SEM; Kruskall-Wallis, $^{**}p < 0.01$ relative to P21; n = 2–4 mice per time point).

patients but also may help with the development of brain-directed treatments for NCLs.

Over the last decade, AAV-mediated gene therapies have been used for several animal models of monogenic retinal degenerations to restore the expression of soluble or transmembrane proteins and to treat vision loss.[8–10] These encouraging studies led to the commencement of clinical trials for inherited retinal degenerative conditions, including Leber congenital amaurosis[11–13] and retinitis pigmentosa.[14] Here we explored the therapeutic potential of an ocular AAV-mediated gene therapy in the $Cln6^{nclf}$ mouse, a naturally occurring model of CLN6 disease, variant late infantile. The mice carry a 1-bp insertion mutation in the *Cln6* gene, which encodes a membrane-bound endoplasmic reticulum (ER) protein of unknown function.[15] The 1-bp insertion results in a frameshift and a truncated short-lived protein product, and it is also found in CLN6 patients of Pakistani origin.[16,17] $Cln6^{nclf}$ mice present with a loss of vision preceding severe neuropathological and behavioral abnormalities.[18,19]

In this study, we show that, although retinal disease in $Cln6^{nclf}$ mice is predominantly characterized by photoreceptor degeneration, supplementation of *CLN6* in photoreceptors is not therapeutic. We also establish that, in unaffected retinas, CLN6 is expressed in photoreceptors and bipolar cells but the level is much higher in bipolar cells. Although bipolar cells are only lost late in disease, AAV-mediated gene delivery of *CLN6* to bipolar cells leads to significantly increased retinal function and long-term preservation of photoreceptors. This study shows that photoreceptor degeneration can be prevented by treating bipolar cells.

RESULTS

CLN6 Is More Highly Expressed in Bipolar Cells Than in Photoreceptors

To determine the potential target cells for gene therapy, we investigated the endogenous expression of the *CLN6* gene in human and mouse retina. Due to the lack of antibodies against the murine protein, we performed immunohistochemical stainings on human retina from non-diseased donor eyes using a previously reported antiserum against human CLN6.[15] We detected a weak fluorescent signal in the outer nuclear layer (ONL) and a strong fluorescent signal in the inner nuclear layer (INL) (Figures 1A, 1B, and 1B"). In the INL, the staining for CLN6 co-localized with staining for PKCα, demonstrating that rod bipolar cells express *CLN6* (Figures 1B and 1B'; Figures S2A–S2B'). Co-staining with an antibody against CRALBP, a marker for Mueller glia cells, did not reveal any co-localization (Figures S2A and S2A'). In the absence of antibodies that could be used for co-localization with CLN6 staining, we were unable to determine what other cell types in the INL expressed the gene. Microarray data on the murine retina suggest that the remaining $CLN6^+$ cells are most likely to be other bipolar cell types, as rod bipolar cells only form a minor fraction of the retinal bipolar cell population.[20]

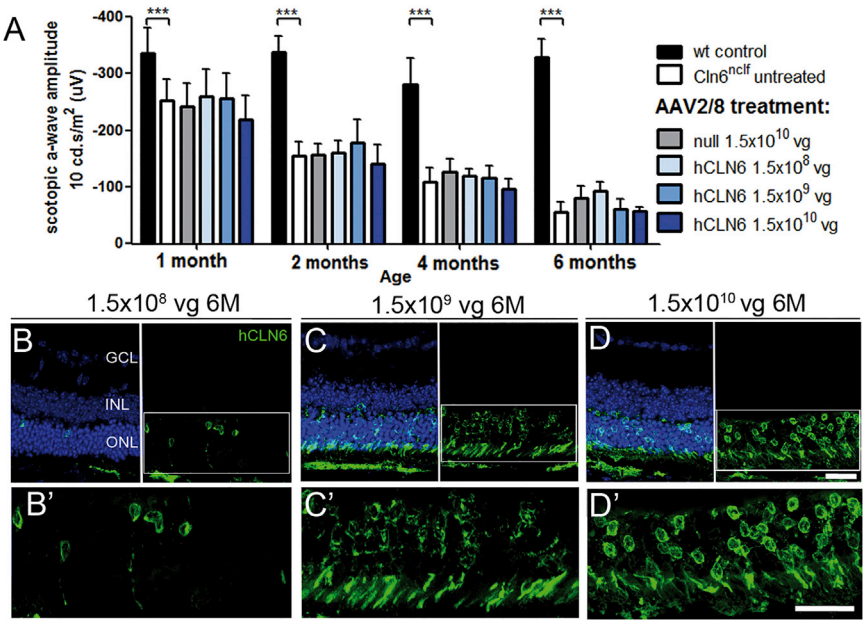

Figure 2. Subretinal Delivery of AAV2/8.CMV.hCLN6 Did Not Rescue Photoreceptors in *Cln6*^{nclf} Mice

(A) Scotopic ERG a-wave amplitudes of *Cln6*^{nclf} mice that received subretinal injections with AAV2/8.CMV.hCLN6 at P9–P11. Wild-type: n = 5–7 eyes, N = 2; *Cln6*^{nclf} untreated: n = 14–17 eyes, N = 5; null: n = 3–4 eyes, N = 1; 1.5×10^8 vg/eye: n = 6 eyes, N = 1; 1.5×10^9 vg/eye: n = 7 eyes, N = 2; 1.5×10^{10} vg/eye: n = 6–8 eyes, N = 2. ***p < 0.001 (2-way ANOVA with Bonferroni post-test). (B–D) hCLN6 staining confirmed transgene expression in photoreceptors at 6 months after transduction with 1.5×10^8 vg/eye (B) and high magnification (B'), 1.5×10^9 vg/eye (C) and high magnification (C'), and 1.5×10^{10} vg/eye (D) and high magnification (D'). Scale bar, 25 μm.

Cln6^{nclf} mice have been reported to present with a predominant loss of photoreceptor function and photoreceptor cells.[18,19] We found that, from post-natal day 21 (P21), retinal function in *Cln6*-deficient mice was progressively compromised under scotopic light conditions, as measured by electroretinography (ERG) recordings (Figures S1A, S1C, and S1D). The photopic ERG was unchanged (Figure S1B). Histological assessment and quantitative analyses of the ONL revealed no severe histological changes at P14 (Figures S1E and S1F). However, *Cln6*^{nclf} mice have a significantly reduced number of photoreceptor nuclei at 1 and 6 months compared with wild-type controls (Figures S1G and S1H). The number of rod bipolar cells in the INL was only reduced in mutant mice at 6 months ($p < 0.001$) (Figures S1I and S1J). In line with previous reports, these data show that *Cln6*^{nclf} mice suffer from an early but mildly progressing rod-mediated retinal degeneration, while loss of rod bipolar cells became only evident at late disease stages.

In the murine retina, we assessed the expression of *Cln6* by real-time qPCR. To confirm the expression of *Cln6* in murine photoreceptors and bipolar cells, we performed real-time qPCRs on mRNA obtained from photoreceptors, sorted via fluorescence-activated cell sorting (FACS) and labeled with the cell surface marker CD73, and rod bipolar cells, labeled with td.tomato in a Pcp2.Cre/td.tomato mouse line (Figures S2B and S2C). In line with the staining on human retina, we found a trend with a higher expression level of *Cln6* in rod bipolar cells than in photoreceptors (Figure 1C). A direct comparison of the absolute number of mRNA molecules by real-time qPCR showed that *Cln6* was expressed to similarly high levels in whole mouse retina as the photoreceptor-specific gene *Peripherin2*, encoding a highly abundant retinal protein[21] (Figure 1D). We studied the relative expression level of *Cln6* in the retina over time using real-time qPCR, and we found that *Cln6* was expressed from birth to adulthood. From P0 to P14, a period when retinal cells undergo post-natal maturation leading to initiation of the phototransduction cascade and eye opening, the expression level of *Cln6* was relatively stable at around 50% of adult levels. At P21 the expression level of *Cln6* increased to the level that was detected in adults (Figure 1E), which may indicate that *Cln6* could play a more important role during vision than during the ocular development.

AAV2/8-Mediated Supplementation of CLN6 in Photoreceptors Is Not Therapeutic in Cln6^{nclf} Mice

We established that *CLN6* was expressed in photoreceptors and that *Cln6* deficiency led to severe loss of photoreceptors in mice, while no early death of bipolar cells was detected in *Cln6*^{nclf} mice despite the high endogenous expression level of *CLN6* in bipolar cells. Consequently, we set out to develop a gene supplementation therapy targeting photoreceptors, and we treated pre-symptomatic P9–P10 *Cln6*^{nclf} mice subretinally with an AAV2/8 vector carrying the ubiquitous cytomegalovirus (CMV) promoter and the human CLN6 (hCLN6) transgene (Figure S3). We administered three different doses ranging from 1.5×10^8 vector genomes (vg)/eye to 1.5×10^{10} vg/eye, and we performed ERG recordings at 1, 2, 4, and 6 months of age. As untreated *Cln6*^{nclf} mice presented with a progressive reduction in rod photoreceptor function, the main functional readout to assess whether the treatment was successful was the scotopic a-wave. None of the treated animals had significantly higher a-wave amplitudes than the untreated or AAV2/8.null vector-treated mutant animals at any time point (Figure 2A). Immunostaining confirmed the presence of the transgene at 6 months. In line with the ERG recordings, the ONL did not appear to be preserved in any of the treated eyes (Figures 2B–2D'; Figure S1G). Further experiments targeting the photoreceptor cells, including earlier treatment at P5 and use of a weak photoreceptor-specific mouse opsin promoter,[22] did not preserve photoreceptor function or improve photoreceptor survival. Since the human and mouse CLN6 protein share about 90% amino acid identity, we also assessed the efficacy of AAV8 carrying mouse *Cln6* and a CMV promoter to exclude that slight differences in the amino acid sequence between human and mouse CLN6 could affect

the outcome of the treatment. No treatment effect was observed (Table S1). These experiments demonstrated that an AAV-mediated gene supplementation therapy targeting photoreceptor cells was not therapeutic in *Cln6*-deficient mice.

The AAV2/2 Variant 7m8 Transduces Bipolar Cells Efficiently in Wild-Type Mice

Conventional AAV serotypes poorly transduce cells in the INL, and bipolar cells are among the cell types least amenable to viral transduction.[23] Several studies have been undertaken to engineer AAV vectors to enhance their transduction efficiency or to increase cell type-specific transduction.[24,25] The recently developed AAV2/2 variant 7m8 was reported to penetrate the retina and transduce cells in all retinal layers following intravitreal delivery in adult mice.[26] To investigate the transduction efficiency of bipolar cells, we produced a 7m8 vector carrying EGFP under the CMV promoter. Wild-type mice received intravitreal injections of the vector at P5, an age before the inner limiting membrane (ILM) is fully established. The ILM can act as a natural barrier in adult animals when AAVs are delivered intravitreally, preventing efficient penetration of viral particles into deep layers of the rodent retina.[27,28] At 3 weeks post-injection, we observed a widespread pan-retinal expression of EGFP (Figure 3A). Higher-magnification images showed strongly transduced ganglion and Mueller glia cells as well as more sparsely transduced photoreceptors (Figure 3C). Immunostaining for PKCα and single confocal images revealed that several rod bipolar cells expressed EGFP (Figures 3B and 3C', white arrows).

To visualize better the transduction of bipolar cells, we injected wild-type animals with a 7m8 vector carrying EGFP under the weak Purkinje cell protein 2 (PCP2) promoter[29] (Figures S4A and S4A') or the 4× enhanced Grm6 (Grm6) promoter,[25] driving expression in rod bipolar cells or all ON bipolar cells, respectively. Magnified single images showed that the majority of PKCα$^+$ bipolar cells and several cone ON bipolar cells (arrowheads) contained EGFP (Figures 3D and 3E). We quantified the proportion of transduced bipolar cells following the administration of 7m8 by flow cytometry. PCP2.Cre/td.tomato mice received intravitreal injections with 7m8.CMV.EGFP at P5 or P6, and we found that approximately 65% of the td.tomato$^+$ rod bipolar cells were positive for EGFP (Figure 3F). We further analyzed the number of transduced photoreceptors, and we established that approximately 25% of the CD73$^+$ photoreceptors expressed EGFP (Figures S4B and S4C). Due to the lack of specific markers labeling all cone bipolar cells, we did not quantify the transduction of other types of bipolar cells.

Intravitreal Delivery of 7m8.CMV.hCLN6 Slowed the Loss of Photoreceptor Function and Photoreceptor Cells in Cln6^{nclf} Mice

ERG recordings, at 1 month following intravitreal injections of 7m8.CMV.hCLN6 in *Cln6*^{nclf} mice at P5–P6, demonstrated that mutant eyes that received a vector dose of 1×10^{10} vg had significantly higher scotopic a-wave amplitudes than untreated eyes or eyes that received 7m8.null control vector. The ERG amplitudes decreased slightly but remained significantly higher in treated than in untreated or 7m8.null-treated eyes at 4, 6, and 9 months. Representative scotopic ERG traces of a mutant mouse that received 1×10^9 vg of 7m8.CMV.hCLN6 in one eye and no treatment in the contralateral eye are shown in Figure 4B, demonstrating the striking difference in retinal function between treated (red traces) and untreated (black traces) eyes at 9 months (see also Figure S5A and Table S2). Histological assessment of the treated eyes at 6 months confirmed the expression of human *CLN6* in cells of all retinal layers. Consistent with the ERG recordings, treated retinas had a thicker ONL, a better structure of photoreceptor outer segment (OS), and reduced activation of Mueller glia cells, as indicated by DAPI, rhodopsin, and glial fibrillary acidic protein (GFAP) staining, respectively (Figure 4C). Counts of DAPI$^+$ photoreceptor nuclei showed that the number of nuclei was higher, with an average of 6 and 7 rows of nuclei in the low-titer and high-titer groups compared with 4 rows in untreated mutant eyes (Figure 4D).

At 6 months, counts of PKCα$^+$ cells did not reveal any significant changes between treated and untreated eyes (Figure 4E). Histological assessment at 9 months confirmed the long-term expression of the therapeutic transgene in treated retinas. It also was apparent that, while the retinal degeneration continued to progress from 6 to 9 months resulting in 2 remaining rows of photoreceptor nuclei in *Cln6*-deficient mice, the number of photoreceptor nuclei was maintained following the 7m8 treatment with 6 and 7 rows of nuclei in the two treatment groups (Figures 4F and 4G). Similarly, the quantification of rod bipolar cells showed that untreated eyes continued to lose PKCα$^+$ cells from 6 to 9 months, whereas treated retinas had significantly higher numbers of rod bipolar cells at 9 months, as highlighted by immunostaining for PKCα (Figures 4F and 4G). We did not maintain any mice for longer than 9 months since motor and behavioral skills, body weight, and survival deteriorated progressively as part of the natural disease progression in *Cln6*-deficient mice.[16]

7m8-Mediated Supplementation of CLN6 in Bipolar Cells Specifically Rescued the Photoreceptor Degeneration in Cln6^{nclf} Mice

To investigate whether the transduction of bipolar cells alone was sufficient to treat the photoreceptor degeneration in *Cln6*-deficient mice, we produced two 7m8.hCLN6 vectors, one carrying the weak PCP2 promoter to drive expression in rod bipolar cells and one carrying the 4× enhanced Grm6 promoter to drive expression in all ON bipolar cells. *Cln6*^{nclf} mice at P5 or P6 received intravitreal injections with either vector at a dose of 1×10^{10} vg/eye. At 4 months, the scotopic a-wave amplitudes were significantly higher in Grm6.hCLN6-treated retinas, reduced slightly over time, but remained significantly higher up to 9 months. Retinas treated with the PCP2.hCLN6 construct showed a weaker therapeutic effect and had significantly increased scotopic a-wave amplitudes only at 6 months (Figure 5A). Figure 5B shows representative scotopic ERG traces of a 9-month-old *Cln6*^{nclf} mouse that received 7m8.Grm6.hCLN6 treatment in one eye and no treatment in the contralateral eye (see also Figure S5B and Table S3). We did not follow up on mice that received injections

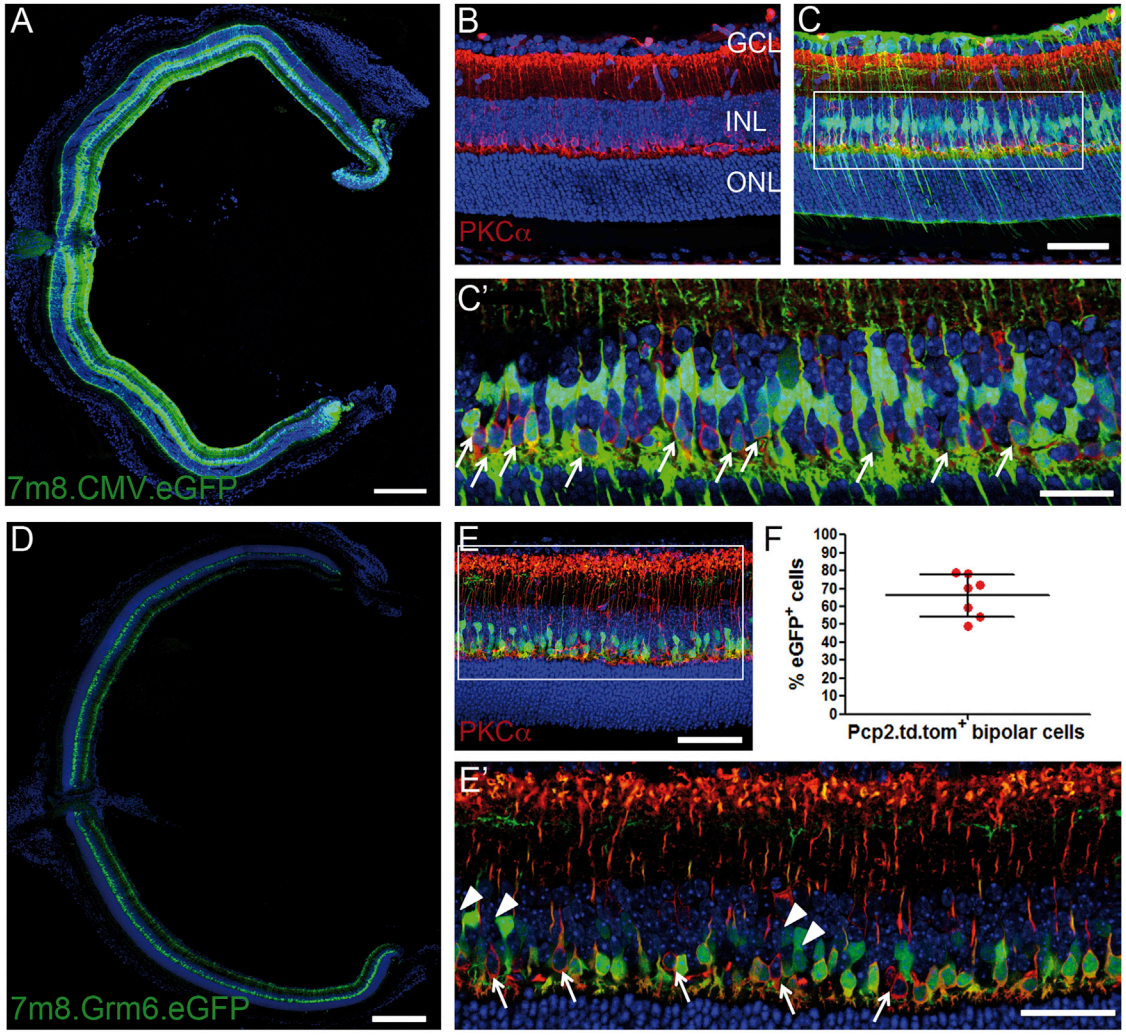

Figure 3. AAV 7m8 Vector Transduced Mouse Bipolar Cells Efficiently

(A) Section of wild-type mouse eye 3 weeks post-intravitreal injection of 1×10^{10} vg 7m8.CMV.EGFP at P5. Scale bar, 250 μm. (B and C) Higher-magnification images of wild-type retinas treated with 7m8.CMV.EGFP and immunostained for PKCα (red) without (B) and with (C) the green channel shown. Scale bar, 50 μm. (C') Single merged image of 7m8.CMV.EGFP-treated wild-type retina showing transduced PKCα$^+$ rod bipolar cells. Scale bar, 25 μm. (D) Section of wild-type mouse eye 3 weeks post-intravitreal injection of 1×10^{10} vg 7m8.Grm6.EGFP at P5. Scale bar, 250 μm. (E) Higher-magnification image of 7m8.Grm6.EGFP-treated retina stained for PKCα (red). Scale bar, 50 μm. (E') Single image demonstrating transduction of the majority of PKCα$^+$ rod bipolar cells (arrows indicate non-transduced PKCα$^+$ cells) and some cone ON bipolar cells (arrowheads), identified by the location of their cell bodies in the INL and synaptic termini in the inner plexiform layer (IPL). Scale bar, 25 μm. (F) Quantification by flow cytometry of the proportion of rod bipolar cells transduced by 7m8 at P5–P6 (mean ± SD; n = 7 eyes).

with 7m8.PCP2.hCLN6 for longer than 6 months in view of the limited beneficial effect.

Analyses of the retinal histology showed that, at 6 months, hCLN6 was present in bipolar cells, rod OS had a better morphology, and Mueller glia cell activation was reduced in PCP2.hCLN6- and Grm6.hCLN6-treated retinas (Figure 5C). Some ganglion cells appeared to express human *CLN6* following the administration of 7m8.Grm6.hCLN6. This was surprising because no expression of EGFP was detected in the ganglion cell layer (GCL) when 7m8.Grm6.EGFP was administered to wild-type mice (see Figures 3D and 3E). Grm6 promoter-driven expression in retinal ganglion cells (RGCs) has been described previously.[30] A possible explanation for the preferential expression of *CLN6* over GFP in the GCL may be that the sequence of the *CLN6* transgene could contain elements that promote the leaky activity of the Grm6 promoter. In agreement with the functional restoration, the thickness of the ONL was increased in both treatment groups, however, this only reached significance in 7m8.Grm6.hCLN6-treated retinas with 6 rows of photoreceptor nuclei compared with 4 rows in untreated mutant retinas at 6 months (Figure 5D). No significant difference in the number of rod bipolar cells was detected following the treatment at 6 months (Figure 5E),

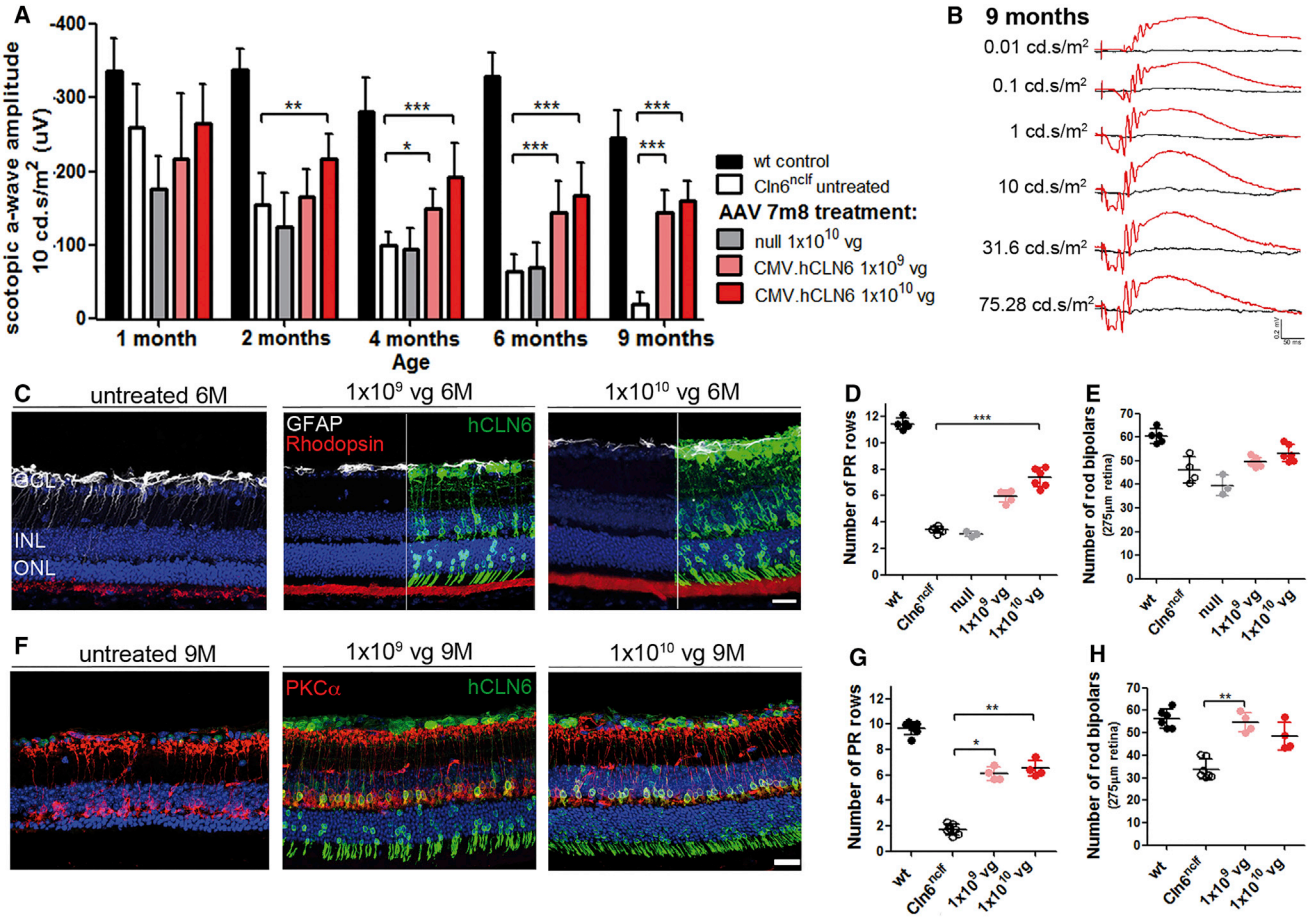

Figure 4. Intravitreal Administration of 7m8.CMV.hCLN6 Slowed Loss of Photoreceptor Function and Photoreceptor Cells in *Cln6*^{nclf} Mice

(A) Scotopic ERG a-wave amplitudes of *Cln6*^{nclf} mice after injection of 7m8.CMV.hCLN6 at P5–P6. Wild-type: n = 5–7 eyes, N = 2; *Cln6*^{nclf} untreated: n = 10–11 eyes (1–6 months), N = 4, n = 5 (9 months), N = 2; null: n = 3–6 eyes, N = 2; 1 × 10^9 vg/eye: n = 11–13 eyes (1–6 months), N = 4, n = 5 (9 months), N = 2; 1 × 10^{10} vg/eye: n = 12 eyes (1–6 months), N = 4, n = 4 (9 months), N = 2. **p < 0.01 and ***p < 0.001 (2-way ANOVA with Bonferroni post-test). (B) Scotopic ERG traces of a *Cln6*^{nclf} mouse 9 months after the administration of 1 × 10^9 vg 7m8.CMV.hCLN6 in one eye (red). Contralateral uninjected eye is in black. (C) hCLN6 staining (green) on treated and untreated eyes at 6 months. GFAP (white) and Rhodopsin (red) showed better morphology in treated eyes. (D) Quantification of photoreceptor rows and (E) PKCα$^+$ cells at 6 months. ***p < 0.001 (Kruskal-Wallis test). (F) hCLN6 (green) and PKCα (red) staining on treated and untreated eyes at 9 months. (G) Quantification of photoreceptor rows and (H) PKCα$^+$ cells at 9 months post-treatment. **p < 0.01 and *p < 0.05 (Kruskal-Wallis test). Scale bars, 25 µm.

but at 9 months the number of PKCα$^+$ cells was significantly increased (p = 0.0057) (Figure 5H), as highlighted by representative images in Figure 5F. From 6 to 9 months, the rows of photoreceptor nuclei remained higher in the treated eyes with 6 rows compared with 2 rows in untreated retinas (p = 0.0025) (Figures 5F and 5G).

DISCUSSION

AAV-mediated gene therapies have proven a successful treatment strategy to combat photoreceptor degenerations in animal models carrying mutations in various genes.[8–10] Here we described the development of a successful treatment for the retinal degeneration in *Cln6*-deficient mice, a model of NCL that carries a mutation in the *Cln6* gene, encoding a transmembrane ER protein of unknown function. We demonstrated that the photoreceptor degeneration in *Cln6*^{nclf} mice was amenable to treatment when the therapeutic *CLN6* transgene was delivered specifically to bipolar cells, a retinal cell type downstream of photoreceptors. The bipolar cells themselves were only lost at late disease stages after the majority of photoreceptors had died. The treatment with the ubiquitous promoter had the biggest beneficial effect, most likely because expression was achieved in all transduced bipolar cell subtypes. The administration of bipolar cell subtype-specific promoter constructs resulted in a slightly lower therapeutic effect. CLN6 deficiency in photoreceptors did not play a central role in the development or progression of the photoreceptor degeneration.

For the successful treatment of the retinal phenotype in *Cln6*^{nclf} mice, it was vital to understand the endogenous expression pattern of *CLN6* in the retina. It was surprising that *CLN6* is more highly expressed in bipolar cells than in photoreceptors, since bipolars are not lost early in disease. Based on our data, a scenario could be envisaged where gene

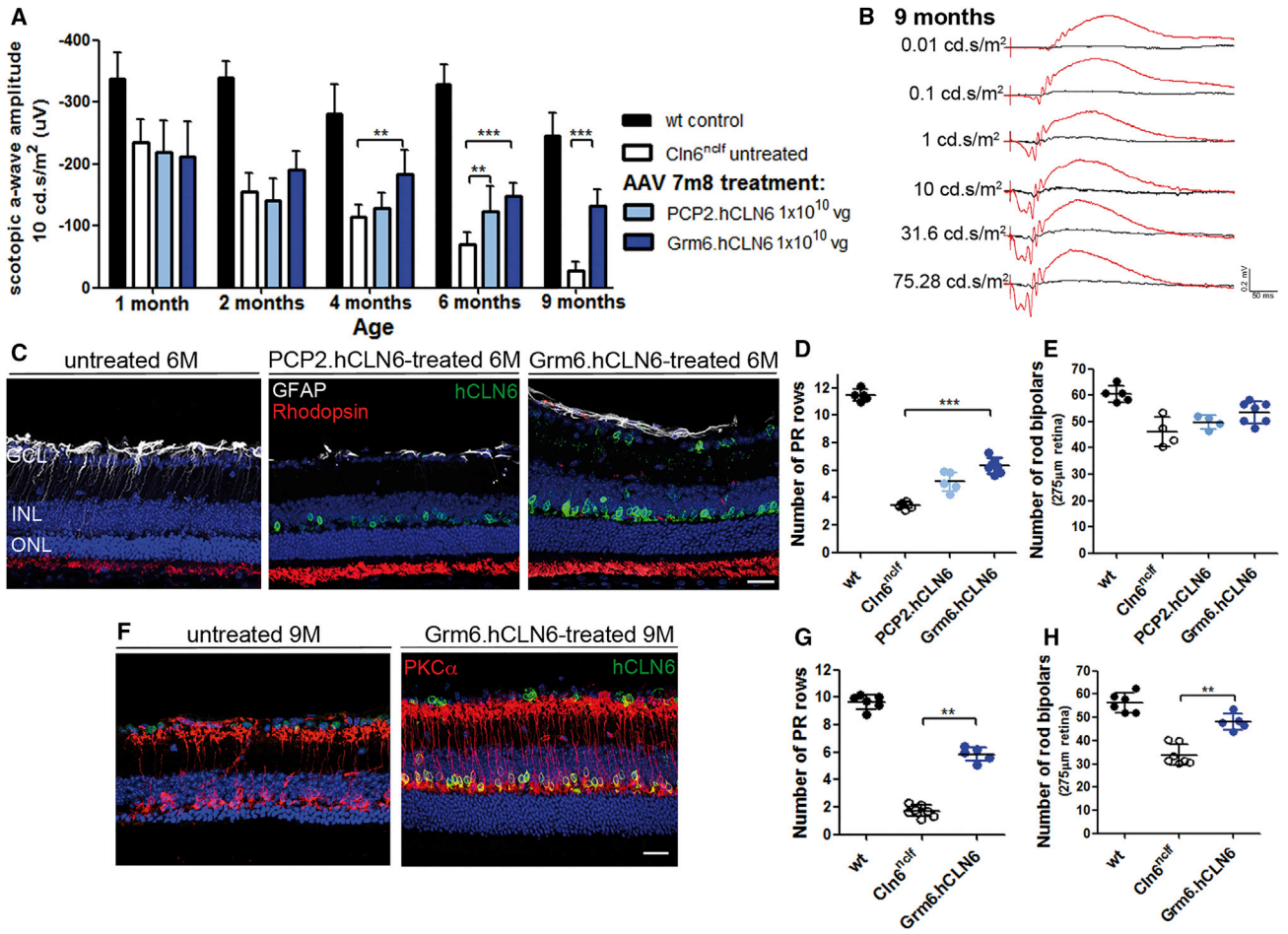

Figure 5. *hCLN6* Delivery to Bipolar Cells Slowed the Loss of Photoreceptor Function and Photoreceptor Cells in *Cln6*^{nclf} Mice

(A) Scotopic ERG a-wave amplitudes of *Cln6*^{nclf} mice after injection of 7m8.PCP2.hCLN6 or 7m8.Grm6.hCLN6 (1×10^{10} vg/eye) at P5–P6. **p < 0.01 and ***p < 0.001 (2-way ANOVA with Bonferroni post-test). Wild-type: n = 5–7 eyes, N = 2; *Cln6*^{nclf} untreated: n = 7–9 eyes (1–6 months), N = 3, n = 5 (9 months), N = 2; PCP2.hCLN6: n = 10–11 eyes, N = 4; Grm6.hCLN6: n = 14 eyes (1–6 months), N = 5, n = 7 (9 months), N = 3. (B) Scotopic ERG traces of a *Cln6*^{nclf} mouse 9 months after the administration of 1×10^{10} vg 7m8.Grm6.hCLN6 in one eye (red). Contralateral uninjected eye is in black. (C) hCLN6 staining (green) on treated and untreated eyes at 6 months confirmed transgene expression in bipolar cells. GFAP (white) and Rhodopsin (red) show better morphology in treated eyes. (D) Quantification of photoreceptor rows and (E) PKCα^{+} cells, 6 months post-treatment. (F) hCLN6 (green) and PKCα (red) staining on treated and untreated eyes at 9 months. (G) Quantification of photoreceptor rows and (H) PKCα^{+} cells at 9 months post-treatment. **p < 0.01 and ***p < 0.001 (Kruskal-Wallis test). Scale bars, 25 µm.

supplementation therapies targeting only the degenerating brain regions or the cell types that are lost early in the disease could be ineffective. Hence, for successful brain-directed gene therapies for CLN6 disease, variant late infantile, it may be necessary to conduct a detailed analysis of the endogenous *CLN6* expression in the different cell types and regions of the brain. While brain-directed gene therapy for CLN6 deficiency using a ubiquitous promoter may be successful and may not require the targeting of specific cells, there is, however, a risk that widespread high-level non-specific expression of CLN6 may result in toxicity. The use of a specific promoter targeting the appropriate cells would decrease that risk.

Retinal disorders arising from defects in bipolar cells are rare. One such disease is complete congenital stationary night blindness (cCSNB), which is caused by mutations in genes expressed in bipolar cells. These lead to a complete loss of the ERG b-wave that is accurately recapitulated in mouse models harboring mutations in genes such as *Grm6* or *Nyctalopin* (Nyx).[31,32] AAV-mediated gene transfer to the bipolar cells of a Nyx-deficient mouse has previously been shown to partially restore bipolar cell function in this stationary disease.[33] In contrast to the phenotype observed in *Cln6*^{nclf} mice, cCSNB does not result in a severe loss of photoreceptors. To our knowledge, this is the first report to describe a retinal dystrophy in which a gene defect in bipolar cells mediates the loss of photoreceptors while leaving the bipolar cells largely unaffected. The ERG recordings performed in our study did not resolve whether the decrease in the scotopic b-wave in untreated *Cln6*^{nclf} mice was a result of the reduced rod photoreceptor function, an intrinsic reduction of rod bipolar cell

function, or a combination of both. Since the b-wave is dependent on the presence of the a-wave, it reflects photoreceptor function, synaptic transmission from photoreceptors to bipolar cells, and bipolar cell function.[34] Therefore, it remains unclear whether bipolar cells, which are not lost at early disease stages in *Cln6*-deficient mice, function normally. It could be speculated that abnormal bipolar cell function could affect the function and viability of photoreceptors as these cells are metabolically very active and sensitive to intra- or extracellular changes,[35] but further studies are required to determine the disease mechanism in *Cln6*-deficient mice.

We have confirmed that in mice the intravitreal administration of the recently developed 7m8 vector in the first post-natal week led to a widespread transgene expression in all retinal layers, including bipolar cells. However, larger animals, such as non-human primates, have a significantly thicker ILM, posing a greater challenge for retinal transduction after intravitreal AAV administration. Following intravitreal injection in non-human primates, transduction by the 7m8 vector appears to be limited to the fovea and retinal areas in close proximity to blood vessels,[26,36] although the efficiency of bipolar cell transduction was not assessed in these studies. It thus remains to be determined whether other vectors and/or approaches are required for efficient targeting of bipolar cells in large animals and for human applications. Alternative vectors able to transduce the bipolar cells in the murine retina have been described, including AAV2/8BP2 and tyrosine-mutated AAVs.[25,37] However, as for AAV 7m8, the efficiency with which these vectors can transduce bipolar cells in larger animals has proved insufficient, making them less attractive for clinical use.[36,37]

The ultimate aim of this study was to investigate whether gene therapy is a potential strategy to treat the retinal degeneration in CLN6 disease, variant late infantile. As lysosomal cross-correction does not occur for CLN6, an ocular AAV-mediated treatment of *Cln6*^{nclf} mice presents a very similar challenge to deficiencies in *CLN3* or other transmembrane defects of NCL. This study therefore also provides a proof of concept of gene therapy for CLN3 disease, juvenile, the most common form of NCL caused by a transmembrane protein defect. Of note is that, once CLN3 disease patients have lost their vision, it can take several years before they develop severe neurological symptoms, creating a time window for therapeutic interventions to treat the visual failure.[38] Recently, mutations in *CLN3* were also linked to cases of non-syndromic retinal degeneration in five unrelated patient families, highlighting further the need for ocular treatments for this condition.[39]

Here we established that endogenous *CLN6* is more highly expressed in bipolar cells than in photoreceptors in mouse and human retinas, consistent with results from a microarray study on the mouse retina.[20] The same microarray study indicates that *Cln3* is expressed in a variety of retinal cell types with a striking abundance only in microglia.[20] In a *Cln3* knockin reporter mouse (*Cln3*$^{lacZ/lacZ}$), X-gal staining was present in bipolar cells as early as P14 and expression in photoreceptors became evident from P21.[40] ERG recordings in *Cln3*-deficient mice showed electronegative retinal responses with a preserved a-wave, an approximately 30% decrease in the b-wave, and no significant cell loss at 12 months.[41] *In vivo* assessment of *Cln3*-deficient mice also revealed that the GCL (including the inner plexiform layer [IPL] and the nerve fiber layer) and the INL were significantly thinner at 18 months than in wild-type mice, while the outer retina measured from the outer plexiform layer (OPL) to OS and from the RPE to the choroid did not show any differences,[42] which may indicate that morphological alterations occur only in the inner retina. In line with these findings, CLN3 disease patients present with an electronegative maximal response and only mild a-wave disturbances at the onset of the disease, pointing to an early inner retinal dysfunction.[38] Collectively, these data indicate that bipolar cells could play an important role, not only in CLN6 disease but also in CLN3 disease. Although *CLN6* and *CLN3* encode for proteins involved in different cellular processes with different subcellular localization,[2] the same strategy to deliver the therapeutic transgene to bipolar cells may be the key to an effective ocular treatment for both diseases.

MATERIALS AND METHODS

Mice

Cln6^{nclf} mice were kindly provided by Professor Thomas Braulke (UKE, Hamburg). C57BL/6J and PCP2.Cre mice were purchased from Harlan Laboratories (UK). PCP2.Cre mice were paired with td.tomato (flox.STOP.flox.td.tomato) mice, and a Cre^{+} litter was confirmed by genotyping. All mice were maintained under cyclic light conditions (12-hr light/dark). If not further specified, the ages of adult mice ranged from 8 to 12 weeks. Animal experiments were performed in accordance with the ARVO Statement for the Use of Animals in Ophthalmic and Vision Research and the UK Home Office license (PPL 70/8120).

Plasmid Construct

The hCLN6 cDNA was cloned into a pD10 vector containing the CMV promoter. To drive expression in rod bipolar cells, the CMV promoter was replaced with the PCP2 promoter kindly provided by Professor John Oberdick (OSU, Ohio). To drive expression in all ON bipolar cells, CLN6 cDNA was cloned into the pD10 vector carrying the 4×Grm6 (4× enhanced mGluR6) promoter kindly provided by Botond Roska (FMI, Basel). To produce a null vector, the pD10 backbone was used carrying an unrelated transgene without promoter and start codon.

Production of rAAV and Intraocular Administration

Recombinant AAV2/8 and 7m8 vector were produced through a triple-transient transfection method and purified by affinity-based AVB Sepharose column (GE Healthcare, UK), as described previously.[43] Viral particle titers were determined by real-time qPCR using primers aligning to the SV40 poly A tail of the genomic plasmid and a specific probe carrying a FAM dye label. Viral vector administration was performed under general anesthesia using an operating microscope (Carl Zeiss) and a 34G needle (Hamilton) as described.[10] A total volume of 1.5 μL or 1 μL recombinant AAV (rAAV) was injected into juvenile (P9–P10) and early post-natal (P5–P6) animals, respectively. At least

two eyes were left uninjected in every mutant cohort, and no animal received the same treatment in left and right eyes.

ERG

ERG recordings were obtained from both eyes in mutant and wild-type animals using commercially available equipment (Espion ERG Diagnosys System), as described previously.[10] After dark adaptation overnight, scotopic examinations were performed under single-flash recording using increasing light intensities. Photopic single-flash recordings were obtained following 5 min of light adaptation at a background light intensity of 30 cd/m^2. N represents the number of independent animal cohorts and n represents the number of eyes in independent animals. ERG data from the same wild-type cohorts are presented in Figures 2, 4, and 5 to provide a reference.

Tissue Preparation

Human paraffin sections of the mid-retina were provided by Dr. Michael Powner (UCL, London). Institutional Review Board (IRB)/Ethics Committee approval was obtained from Dr. Marcus Fruttiger (UCL, London). The tissue was fixed in 2% paraformaldehyde (PFA) and obtained as described previously.[44] 6-μm-thick retinal sections were deparaffinized in xylene substitute (Sigma-Aldrich) and rehydrated in alcohol gradients of 100%, 75%, 50%, and 30%, followed by a final PBS wash. For antibody staining, the slides were heated to 120°C in 90% glycerol and 10% citrate buffer (pH 6.0). For mouse retinal sections, the murine eyes were enucleated following cervical dislocation, and cornea, iris, and lens were removed. The eye cups were fixed in 4% PFA for 1–2 hr, cryoprotected in 20% sucrose, and flash-frozen in embedding matrix OCT.

Immunohistochemistry

The slides were briefly washed in PBS and blocking buffer was employed containing 5% normal goat serum (NGS), 1% BSA, and 0.1% Triton X-100. The samples were incubated in primary antibody diluted in blocking buffer at 4°C overnight. Sections were washed in PBS and incubated in secondary antibody diluted in blocking buffer. Subsequently sections were washed in PBS, washed with 600 nM DAPI for 5 min, and mounted in DAKO mounting media. The slides were stored in the dark at 4°C until imaging by confocal microscopy (Leica DM5500Q).

Quantification of Retinal Cross Sections

Eyes were sectioned in a sagittal orientation (18 μm) and collected on glass slides. Confocal images (275 × 275 μm) were taken from the superior and inferior midcentral retina of three sagittal cross sections on each slide. To assess the ONL thickness, three vertical columns of DAPI$^+$ photoreceptor nuclei were counted in each of the six single confocal images. The counts of PKCα$^+$ cells were performed on the corresponding projection images. PKCα counts in Figure S1 were performed on stained sections using mouse anti-PKCα antibody (Sigma-Aldrich). For all other PKCα counts, staining was performed using mouse anti-PKCα antibody (Santa Cruz Biotechnology). Counts included age-matched wild-type controls. Researchers performing counts were masked to the genotype of the animals and treatment received.

Real-Time qRT-PCR

Total RNA was extracted from mouse retinas or cell samples sorted via FACS using the RNeasy Mini Kit (QIAGEN). The QuantiTect Reverse Transcription Kit (QIAGEN) was utilized to generate cDNA. qRT-PCRs were performed in 96-well plates in a PCR thermal cycler (Applied Biosciences 7900HT) using a 2× FastStart TagMan Probe Mastermix assay (Roche) with a probe concentration of 100 nm and a primer concentration of 200 nm with the following primers:

forward β-actin (5′-AAGGCCAACCGTGAAAAGAT-3′),

reverse β-actin (5′-GTGGTACGACCAGAGGCATAC-3′),

forward Cln6 (5′-AGAGCCACATGCCAGGAC-3′),

reverse Cln6 (5′-GGCGAAGAAGGTGAAGATGA-3′),

forward Peripherin2 (5′-TGGATCAGCAATCGCTACCT-3′), and

reverse Peripherin2 (5′-CCATCCACGTTGCTCTTGA-3′).

Triplicate reactions were carried out for each sample. The Ct values were calculated using the computer program SDS 2.2.2 (Applied Biosciences). To determine relative expression levels, the Ct values of the triplicate reactions for every gene were averaged and normalized to the averaged β-actin Ct values of each corresponding sample (ΔCt). For absolute quantification, a dilution series of plasmid DNA ranging from 1.5×10^3 to 1.5×10^7 molecules was used to produce a standard curve. A dilution series of wild-type mouse retina cDNA was performed in the ratios of 1:10:100. The obtained Ct values were averaged per triplicate reaction, and the number of specific cDNA molecules per nanogram total mRNA was calculated by standard curve intrapolation.

Retinal Semithin Sections

Eyes were enucleated and the cornea and lens removed. The eyecups were fixed in Karnovsky fixative for at least 30 hr at 4°C. The eyes were dehydrated by passage through ascending ethanol series (50%–100%) and propylene oxide, and they were infiltrated overnight with a 1:1 mixture of propylene oxide: Epoxy resin. After a further 8 hr in full resin, eyes were embedded in fresh resin and incubated overnight at 60°C. Semithin (0.7-μm) sections were cut in the inferior-superior axis passing through the optic nerve head using a Leica ultracut S microtome. Retinal semithin sections were stained with a 1% mixture of toluidine blue-borax in 50% ethanol. Images were captured of the inferior and superior mid-retina from three sections per eye (in total six images per eye) using a Qimaging camera (MicroPublisher 5.0 RT) mounted on a light microscope (Leica DM IRB). Images were exported as .tif files and measurements were performed in ImageJ.

FACS and Flow Cytometry Analysis

Cell sorting was performed using a BD Influx Cell Sorter (BD Biosciences, USA) fitted with a 200-mW 488-nm blue laser that was used to excite GFP detected in the 488- to 530/40-nm channel, a 50-mW 561-nm yellow/green laser that was used to excite tdTomato detected

in the 561- to 585/29-nm channel, and a 100-mW 640-nm red laser used to excite an anti-mouse CD73-APC antibody (BioLegend, 127209) detected in the 640- to 670/30-nm channel. Sorting of photoreceptors and bipolar cells was performed with a 70-μm nozzle at 50 psi. To determine cell viability, DRAQ7 (Biostatus, DR71000) dead cell stain was added to the samples at a final concentration of 0.6 μM for 5 min at room temperature. All of the samples were analyzed using a BD LSRFortessa^{TM} X-20 flow cytometer (BD Biosciences, USA) fitted with 5 lasers (i.e., 355-, 405-, 488-, 561-, and 640-nm lasers). Results were subsequently analyzed using FlowJo software version (v.)9.9.5.

Statistical Analysis

Data are represented as means ± SD or ± SEM with the appropriate n (number of independent samples) values as indicated. The appropriate tests and p values are provided in the figure legends with *$p < 0.05$, **$p < 0.01$, and ***$p < 0.001$.

SUPPLEMENTAL INFORMATION

Supplemental Information includes five figures and three tables and can be found with this article online at https://doi.org/10.1016/j.ymthe.2018.02.027.

AUTHOR CONTRIBUTIONS

S.-M.k.H., J.R., L.A.-H., R.A.P., Y.D., A.G., R.D.S., and J.H. planned and conducted the experiments. S.-M.K.H., R.D.S., and A.J.S. analyzed the data. R.A.P., Y.D., A.G., R.D.S., M.R., R.M., S.A., U.F.O.L., A.J.S., S.E.M., and R.R.A. provided expertise and feedback. A.J.S., S.E.M., and R.R.A. secured funding and supervised the study. S.-M.k.H., A.J.S., S.E.M., and R.R.A. conceptualized the study and wrote the paper.

CONFLICTS OF INTEREST

U.F.O.L. is an employee of F. Hoffmann-La Roche Ltd. The remaining authors do not declare any conflicts of interest.

ACKNOWLEDGMENTS

We thank Professor Thomas Braulke for the *Cln6*^{nclf} mouse line and Dr. Michael Powner for providing non-diseased human retinal tissue. This project was supported by the Batten Disease Family Association, charity No 1084908, Beefy's Charity Foundation, the European Union's Horizon 2020 research and innovation programme (grant 66691), the European Union Seventh Framework Programme (FP7/2007–2013, grant 281234), RP Fighting Blindness (grant GR576), and Moorfields Eye Charity and Medical Research Council. R.R.A. is partially supported by the NIHR Biomedical Research Centre at Moorfields Eye Hospital and the UCL Institute of Ophthalmology.

REFERENCES

1. Mole, S., Williams, R., and Goebel, H. (2011). The Neuronal Ceroid Lipofuscinoses (Batten Disease), Second Edition (Oxford University Press).
2. Kollmann, K., Uusi-Rauva, K., Scifo, E., Tyynelä, J., Jalanko, A., and Braulke, T. (2013). Cell biology and function of neuronal ceroid lipofuscinosis-related proteins. Biochim. Biophys. Acta *1832*, 1866–1881.
3. Sands, M.S., and Davidson, B.L. (2006). Gene therapy for lysosomal storage diseases. Mol. Ther. *13*, 839–849.
4. Consortium, T.I.B.D.; The International Batten Disease Consortium (1995). Isolation of a novel gene underlying Batten disease, CLN3. Cell *82*, 949–957.
5. Schulz, A., Kohlschütter, A., Mink, J., Simonati, A., and Williams, R. (2013). NCL diseases - clinical perspectives. Biochim. Biophys. Acta *1832*, 1801–1806.
6. Sondhi, D., Scott, E.C., Chen, A., Hackett, N.R., Wong, A.M.S., Kubiak, A., Nelvagal, H.R., Pearse, Y., Cotman, S.L., Cooper, J.D., and Crystal, R.G. (2014). Partial correction of the CNS lysosomal storage defect in a mouse model of juvenile neuronal ceroid lipofuscinosis by neonatal CNS administration of an adeno-associated virus serotype rh.10 vector expressing the human CLN3 gene. Hum. Gene Ther. *25*, 223–239.
7. Bosch, M.E., Aldrich, A., Fallet, R., Odvody, J., Burkovetskaya, M., Schuberth, K., Fitzgerald, J.A., Foust, K.D., and Kielian, T. (2016). Self-Complementary AAV9 Gene Delivery Partially Corrects Pathology Associated with Juvenile Neuronal Ceroid Lipofuscinosis (CLN3). J. Neurosci. *36*, 9669–9682.
8. Komáromy, A.M., Alexander, J.J., Rowlan, J.S., Garcia, M.M., Chiodo, V.A., Kaya, A., Tanaka, J.C., Acland, G.M., Hauswirth, W.W., and Aguirre, G.D. (2010). Gene therapy rescues cone function in congenital achromatopsia. Hum. Mol. Genet. *19*, 2581–2593.
9. Carvalho, L.S., Xu, J., Pearson, R.A., Smith, A.J., Bainbridge, J.W., Morris, L.M., Fliesler, S.J., Ding, X.Q., and Ali, R.R. (2011). Long-term and age-dependent restoration of visual function in a mouse model of CNGB3-associated achromatopsia following gene therapy. Hum. Mol. Genet. *20*, 3161–3175.
10. Nishiguchi, K.M., Carvalho, L.S., Rizzi, M., Powell, K., Holthaus, S.-M.K., Azam, S.A., Duran, Y., Ribeiro, J., Luhmann, U.F., Bainbridge, J.W., et al. (2015). Gene therapy restores vision in rd1 mice after removal of a confounding mutation in Gpr179. Nat. Commun. *6*, 6006.
11. Testa, F., Maguire, A.M., Rossi, S., Pierce, E.A., Melillo, P., Marshall, K., Banfi, S., Surace, E.M., Sun, J., Acerra, C., et al. (2013). Three-year follow-up after unilateral subretinal delivery of adeno-associated virus in patients with Leber congenital Amaurosis type 2. Ophthalmology *120*, 1283–1291.
12. Bainbridge, J.W.B., Mehat, M.S., Sundaram, V., Robbie, S.J., Barker, S.E., Ripamonti, C., Georgiadis, A., Mowat, F.M., Beattie, S.G., Gardner, P.J., et al. (2015). Long-term effect of gene therapy on Leber's congenital amaurosis. N. Engl. J. Med. *372*, 1887–1897.
13. Weleber, R.G., Pennesi, M.E., Wilson, D.J., Kaushal, S., Erker, L.R., Jensen, L., McBride, M.T., Flotte, T.R., Humphries, M., Calcedo, R., et al. (2016). Results at 2 Years after Gene Therapy for RPE65-Deficient Leber Congenital Amaurosis and Severe Early-Childhood-Onset Retinal Dystrophy. Ophthalmology *123*, 1606–1620.
14. Ghazi, N.G., Abboud, E.B., Nowilaty, S.R., Alkuraya, H., Alhommadi, A., Cai, H., Hou, R., Deng, W.T., Boye, S.L., Almaghamsi, A., et al. (2016). Treatment of retinitis pigmentosa due to MERTK mutations by ocular subretinal injection of adeno-associated virus gene vector: results of a phase I trial. Hum. Genet. *135*, 327–343.
15. Mole, S.E., Michaux, G., Codlin, S., Wheeler, R.B., Sharp, J.D., and Cutler, D.F. (2004). CLN6, which is associated with a lysosomal storage disease, is an endoplasmic reticulum protein. Exp. Cell Res. *298*, 399–406.
16. Bronson, R.T., Donahue, L.R., Johnson, K.R., Tanner, A., Lane, P.W., and Faust, J.R. (1998). Neuronal ceroid lipofuscinosis (nclf), a new disorder of the mouse linked to chromosome 9. Am. J. Med. Genet. *77*, 289–297.
17. Gao, H., Boustany, R.-M.N., Espinola, J.A., Cotman, S.L., Srinidhi, L., Antonellis, K.A., Gillis, T., Qin, X., Liu, S., Donahue, L.R., et al. (2002). Mutations in a novel CLN6-encoded transmembrane protein cause variant neuronal ceroid lipofuscinosis in man and mouse. Am. J. Hum. Genet. *70*, 324–335.
18. Mirza, M., Volz, C., Karlstetter, M., Langiu, M., Somogyi, A., Ruonala, M.O., Tamm, E.R., Jägle, H., and Langmann, T. (2013). Progressive retinal degeneration and glial activation in the CLN6 (nclf) mouse model of neuronal ceroid lipofuscinosis: a beneficial effect of DHA and curcumin supplementation. PLoS ONE *8*, e75963.
19. Bartsch, U., Galliciotti, G., Jofre, G.F., Jankowiak, W., Hagel, C., and Braulke, T. (2013). Apoptotic photoreceptor loss and altered expression of lysosomal proteins in the nclf mouse model of neuronal ceroid lipofuscinosis. Invest. Ophthalmol. Vis. Sci. *54*, 6952–6959.

20. Siegert, S., Cabuy, E., Scherf, B.G., Kohler, H., Panda, S., Le, Y.-Z., Fehling, H.J., Gaidatzis, D., Stadler, M.B., and Roska, B. (2012). Transcriptional code and disease map for adult retinal cell types. Nat. Neurosci. *15*, 487–495, S1–S2.

21. Travis, G.H., Sutcliffe, J.G., and Bok, D. (1991). The retinal degeneration slow (rds) gene product is a photoreceptor disc membrane-associated glycoprotein. Neuron *6*, 61–70.

22. Pawlyk, B.S., Smith, A.J., Buch, P.K., Adamian, M., Hong, D.-H., Sandberg, M.A., Ali, R.R., and Li, T. (2005). Gene replacement therapy rescues photoreceptor degeneration in a murine model of Leber congenital amaurosis lacking RPGRIP. Invest. Ophthalmol. Vis. Sci. *46*, 3039–3045.

23. Dalkara, D., and Sahel, J.-A. (2014). Gene therapy for inherited retinal degenerations. C. R. Biol. *337*, 185–192.

24. Kay, C.N., Ryals, R.C., Aslanidi, G.V., Min, S.-H., Ruan, Q., Sun, J., Dyka, F.M., Kasuga, D., Ayala, A.E., Van Vliet, K., et al. (2013). Targeting photoreceptors via intravitreal delivery using novel, capsid-mutated AAV vectors. PLoS ONE *8*, e62097.

25. Cronin, T., Vandenberghe, L.H., Hantz, P., Juttner, J., Reimann, A., Kacsó, A.E., Huckfeldt, R.M., Busskamp, V., Kohler, H., Lagali, P.S., et al. (2014). Efficient transduction and optogenetic stimulation of retinal bipolar cells by a synthetic adeno-associated virus capsid and promoter. EMBO Mol. Med. *6*, 1175–1190.

26. Dalkara, D., Byrne, L.C., Klimczak, R.R., Visel, M., Yin, L., Merigan, W.H., Flannery, J.G., and Schaffer, D.V. (2013). In vivo-directed evolution of a new adeno-associated virus for therapeutic outer retinal gene delivery from the vitreous. Sci. Transl. Med. *5*, 189ra76.

27. Harvey, A.R., Kamphuis, W., Eggers, R., Symons, N.A., Blits, B., Niclou, S., Boer, G.J., and Verhaagen, J. (2002). Intravitreal injection of adeno-associated viral vectors results in the transduction of different types of retinal neurons in neonatal and adult rats: a comparison with lentiviral vectors. Mol. Cell. Neurosci. *21*, 141–157.

28. Dalkara, D., Kolstad, K.D., Caporale, N., Visel, M., Klimczak, R.R., Schaffer, D.V., and Flannery, J.G. (2009). Inner limiting membrane barriers to AAV-mediated retinal transduction from the vitreous. Mol. Ther. *17*, 2096–2102.

29. Oberdick, J., Smeyne, R.J., Mann, J.R., Zackson, S., and Morgan, J.I. (1990). A promoter that drives transgene expression in cerebellar Purkinje and retinal bipolar neurons. Science *248*, 223–226.

30. van Wyk, M., Hulliger, E.C., Girod, L., Ebneter, A., and Kleinlogel, S. (2017). Present Molecular Limitations of ON-Bipolar Cell Targeted Gene Therapy. Front. Neurosci. *11*, 161.

31. Masu, M., Iwakabe, H., Tagawa, Y., Miyoshi, T., Yamashita, M., Fukuda, Y., Sasaki, H., Hiroi, K., Nakamura, Y., Shigemoto, R., et al. (1995). Specific deficit of the ON response in visual transmission by targeted disruption of the mGluR6 gene. Cell *80*, 757–765.

32. Pardue, M.T., McCall, M.A., LaVail, M.M., Gregg, R.G., and Peachey, N.S. (1998). A naturally occurring mouse model of X-linked congenital stationary night blindness. Invest. Ophthalmol. Vis. Sci. *39*, 2443–2449.

33. Scalabrino, M.L., Boye, S.L., Fransen, K.M.H., Noel, J.M., Dyka, F.M., Min, S.-H., Ruan, Q., De Leeuw, C.N., Simpson, E.M., Gregg, R.G., et al. (2015). Intravitreal delivery of a novel AAV vector targets ON bipolar cells and restores visual function in a mouse model of complete congenital stationary night blindness. Hum. Mol. Genet. *24*, 6229–6239.

34. Stockton, R.A., and Slaughter, M.M. (1989). B-wave of the electroretinogram. A reflection of ON bipolar cell activity. J. Gen. Physiol. *93*, 101–122.

35. Wong-Riley, M. (2010). Energy metabolism of the visual system. Eye Brain *2*, 99–116.

36. Ramachandran, P.S., Lee, V., Wei, Z., Song, J.Y., Casal, G., Cronin, T., Willett, K., Huckfeldt, R., Morgan, J.I., Aleman, T.S., et al. (2017). Evaluation of dose and safety of AAV7m8 and AAV8BP2 in the non-human primate retina. Hum. Gene Ther. *28*, 154–167.

37. Mowat, F.M., Gornik, K.R., Dinculescu, A., Boye, S.L., Hauswirth, W.W., Petersen-Jones, S.M., and Bartoe, J.T. (2014). Tyrosine capsid-mutant AAV vectors for gene delivery to the canine retina from a subretinal or intravitreal approach. Gene Ther. *21*, 96–105.

38. Collins, J., Holder, G.E., Herbert, H., and Adams, G.G.W. (2006). Batten disease: features to facilitate early diagnosis. Br. J. Ophthalmol. *90*, 1119–1124.

39. Wang, F., Wang, H., Tuan, H.-F., Nguyen, D.H., Sun, V., Keser, V., Bowne, S.J., Sullivan, L.S., Luo, H., Zhao, L., et al. (2014). Next generation sequencing-based molecular diagnosis of retinitis pigmentosa: identification of a novel genotype-phenotype correlation and clinical refinements. Hum. Genet. *133*, 331–345.

40. Ding, S.-L., Tecedor, L., Stein, C.S., and Davidson, B.L. (2011). A knock-in reporter mouse model for Batten disease reveals predominant expression of Cln3 in visual, limbic and subcortical motor structures. Neurobiol. Dis. *41*, 237–248.

41. Staropoli, J.F., Haliw, L., Biswas, S., Garrett, L., Hölter, S.M., Becker, L., Skosyrski, S., Da Silva-Buttkus, P., Calzada-Wack, J., Neff, F., et al. (2012). Large-scale phenotyping of an accurate genetic mouse model of JNCL identifies novel early pathology outside the central nervous system. PLoS One *7*, e38310.

42. Groh, J., Stadler, D., Buttmann, M., and Martini, R. (2014). Non-invasive assessment of retinal alterations in mouse models of infantile and juvenile neuronal ceroid lipofuscinosis by spectral domain optical coherence tomography. Acta Neuropathol. Commun. *2*, 54.

43. Davidoff, A.M., Ng, C.Y.C., Sleep, S., Gray, J., Azam, S., Zhao, Y., McIntosh, J.H., Karimipoor, M., and Nathwani, A.C. (2004). Purification of recombinant adeno-associated virus type 8 vectors by ion exchange chromatography generates clinical grade vector stock. J. Virol. Methods *121*, 209–215.

44. Powner, M.B., Gillies, M.C., Tretiach, M., Scott, A., Guymer, R.H., Hageman, G.S., and Fruttiger, M. (2010). Perifoveal müller cell depletion in a case of macular telangiectasia type 2. Ophthalmology *117*, 2407–2416.

YMTHE, Volume *26*

Supplemental Information

Prevention of Photoreceptor Cell Loss in a *Cln6*^{nclf} Mouse Model of Batten Disease Requires *CLN6* Gene Transfer to Bipolar Cells

Sophia-Martha kleine Holthaus, Joana Ribeiro, Laura Abelleira-Hervas, Rachael A. Pearson, Yanai Duran, Anastasios Georgiadis, Robert D. Sampson, Matteo Rizzi, Justin Hoke, Ryea Maswood, Selina Azam, Ulrich F.O. Luhmann, Alexander J. Smith, Sara E. Mole, and Robin R. Ali

Supporting information – Results

Table S1: Summary of all subretinal AAV2/8 injections performed in *Cln6*^{nclf} mice. Mean ± SD of the scotopic a-wave amplitudes (at 10 cd.s/m^2, 2 months post-treatment), the main functional readout for the therapeutic effect, did not show a significant increase in rod photoreceptor function in treated *Cln6*^{nclf} eyes. Mean scotopic a-wave amplitudes of the contralateral untreated *Cln6*^{nclf} eyes and wild type mice are provided for reference. N = number of independent animal cohorts, *n* = number of eyes in independent animals.

Treatment age	Promoter and transgene	Titre	Scotopic a-wave amplitudes (mean ±SD)	*n*	N
P9-P10	CMV.hCLN6	1.5x10^{10} vg/eye	-140.53 ±33.34	8	2
P9-P10	CMV.hCLN6	1.5x10^{9} vg/eye	-178.41 ±40.72	7	2
P10	CMV.hCLN6	1.5x10^{8} vg/eye	-159.81 ±22.38	6	1
P5	CMV.hCLN6	1x10^{9} vg/eye	-125.91 ±23.29	5	2
P5	CMV.hCLN6	1x10^{8} vg/eye	-152.06 ±35.75	5	2
P9	CMV.mCln6	1.5x10^{9} vg/eye	-103.68 ±25.85	5	1
P9	CMV.mCln6	1.5x10^{8} vg/eye	-152.30 ±14.86	3	1
P10	MOPS.hCLN6	1.5x10^{11} vg/eye	-100.96 ±11.56	3	1
P9	MOPS.hCLN6	1.5x10^{10} vg/eye	-105.62 ±21.54	6	1
P9-P10	MOPS.hCLN6	1.5x10^{9} vg/eye	-147.27 ±71.89	5	2
P9	null control	1.5x10^{10} vg/eye	-157.27 ±19.29	4	1
Untreated *Cln6*^{nclf}	-	-	-145.06 ±30.99	47	9
WT C57BL/6J	-	-	-338.44 ±24.19	7	1

Table S2: Summary of mice used for the ERG recordings following the treatment with 7m8.CMV.hCLN6 (as shown in figure 4). N = number of independent animal cohorts, *n* = number of eyes in independent animals.

Treatment age	**Promoter and transgene**	**Titre**	***n* at 1-6 months**				**N**	***n***	**N**
			1M	2M	4M	6M	1M-6M	9M	9M
P5-P6	CMV.hCLN6	$1x10^{10}$ vg/eye	12	12	12	12	4	4	2
P5-P6	CMV.hCLN6	$1x10^{19}$ vg/eye	12	13	13	11	4	5	2
P5-P6	null control	$1x10^{10}$ vg/eye	3	6	6	5	2	-	-
Untreated *Cln6*^{nclf}	-	-	10	10	11	11	4	5	2
WT C57BL/6J	-	-	7	5	6	5	2	7	1

Table S3: Summary of mice used for the ERG recordings following the treatment with 7m8.Grm6.hCLN6 and 7m8.PCP2.hCLN6 (as shown in figure 5). N = number of independent animal cohorts, *n* = number of eyes in independent animals.

Treatment age	**Promoter and transgene**	**Titre**	***n* at 1-6 months**				**N**	***n***	**N**
			1M	2M	4M	6M	1M-6M	9M	9M
P5-P6	PCP2.hCLN6	$1x10^{10}$ vg/eye	11	11	10	10	4	-	-
P5-P6	Grm6.hCLN6	$1x10^{10}$ vg/eye	14	14	14	14	5	7	3
Untreated *Cln6*^{nclf}	-	-	7	7	9	9	3	5	2
WT C57BL/6J	-	-	7	5	6	5	2	7	1

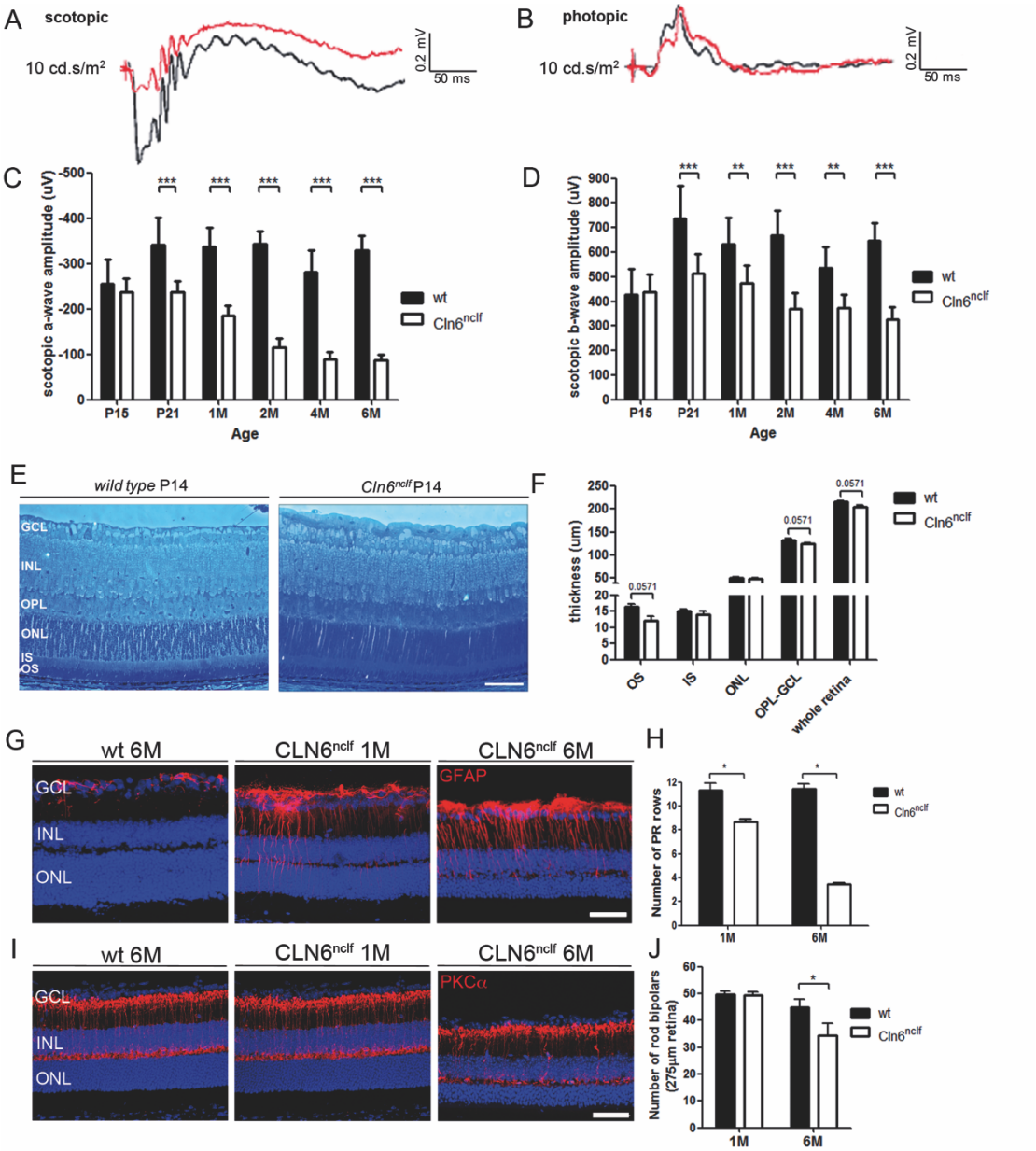

Figure S1: Characterisation of the ocular phenotype in *Cln6*^{nclf} mice. Representative (A) scotopic and (B) photopic ERG traces at 10 cd.s/m from wild type (black) and *Cln6*^{nclf} (red) mice at 2 months. (C) Scotopic a-wave and (D) b-wave amplitudes from right eyes at 10 cd.s/m^2 over time (means ± SD). *Cln6*^{nclf}: n = 6-10 eyes, wild type: n = 5-7 eyes per time point. (E) Representative images of semithin retinal sections revealed no obvious morphological abnormalities, (F) no significant differences were detected in the thickness of the retina at P14 in mutant and wild type mice. A non-parametric Mann-Whitney U test was performed. *Cln6*^{nclf} n = 3 eyes, wild type n = 4 eyes. (G) Mueller glia cell activation indicated by increased GFAP staining (red) and loss of photoreceptors labelled with DAPI nuclear staining (blue) were present from 1 month in mutant retinas. (H) At 1 month and 6 months the number of photoreceptor rows was significantly decreased in mutant mice (means ± SD), n = 5 eyes per group. (I) Immunostaining for PKCα (red) highlighted a mild loss of rod bipolar cells at 6 months. (J) The number of PKCα positive cells was reduced in *Cln6*^{nclf} mice at 6 months but not at 1 month (means ± SD). *Cln6*^{nclf}: n = 5 eyes, wild type: n = 4 eyes. Two-way ANOVA with Bonferroni post-test were performed to determine significance between wild type and *Cln6*^{nclf} mice. $p < 0.01$ = **, $p < 0.001$ = ***. P = postnatal day, M = month, GCL = ganglion cell layer, INL = inner nuclear layer, OPL = outer plexiform layer, ONL = outer nuclear layer, OS = outer segments, IS = inner segments. Scale bars 50 μm.

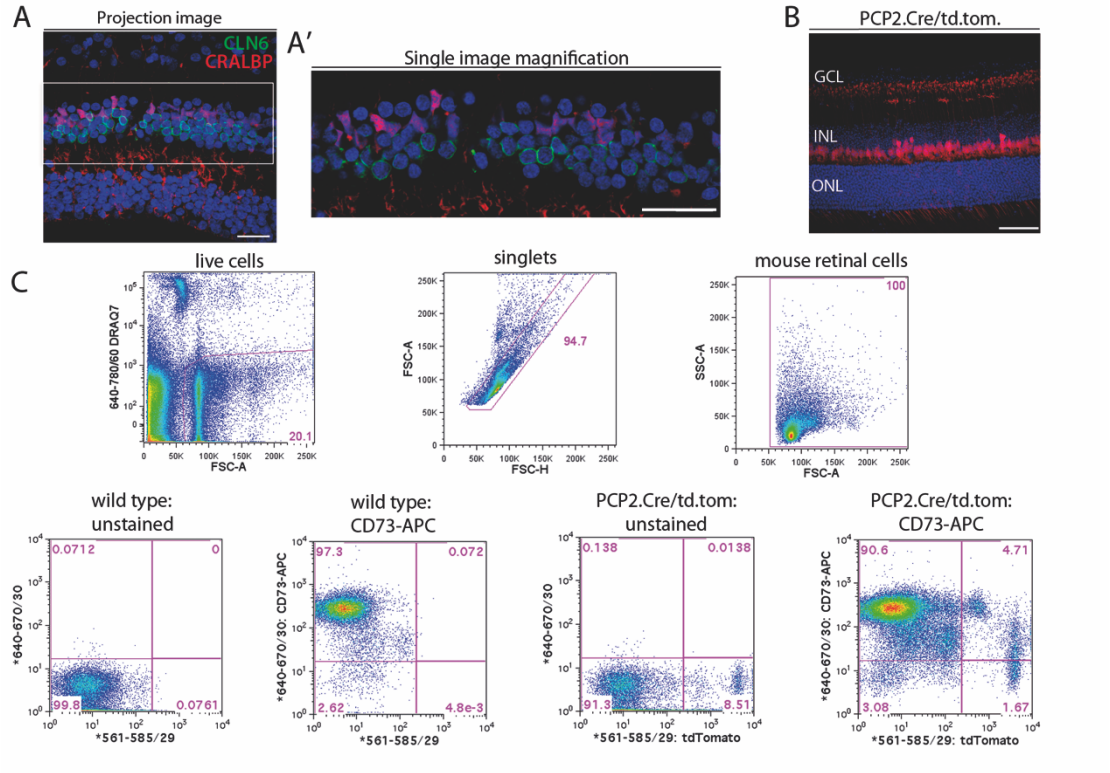

Figure S2: Assessment of CLN6 in inner retinal cells

(A-B') Immunostaining for CLN6 (green) and PKCα (red) on human retinal cross-section showing that CLN6 is expressed in rod bipolar cells. (C-C') Staining for CLN6 (green) and CRALBP (red) showing that CLN6 is not expressed in Mueller glia cells. (D) Representative retinal cross-section of a PCP2.Cre/td.tomato mouse. Following the pairing of PCP2.Cre and flox.STOP.flox.td.tomato mice, the retinas of the Cre-positive offspring were used for further analysis. Td.tomato expression was detected in bipolar cells and also in photoreceptors. (E) FACS-gating strategy to isolate CD73-positive photoreceptors and td.tomato-positive/CD73-negative bipolar cells to extract cell type specific RNA for qPCR analyses. Scale bars 50 µm.

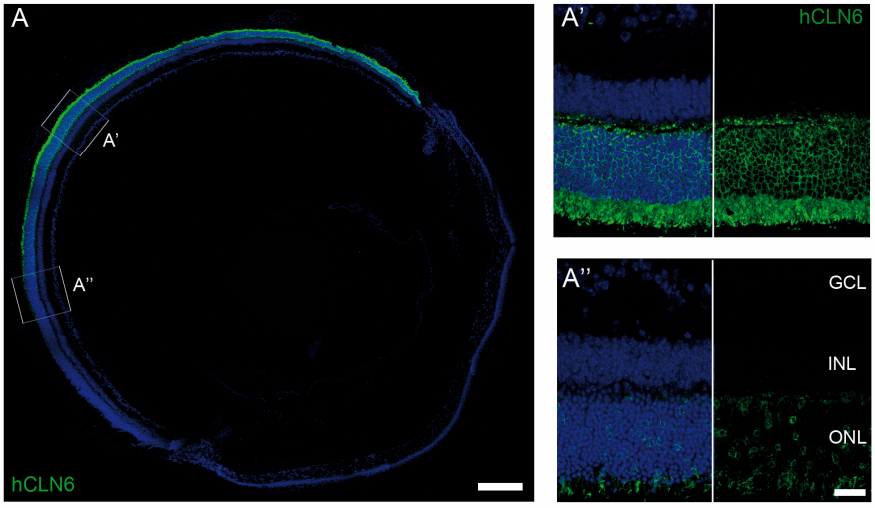

Figure S3: Subretinal administration of AAV2/8 in wild type retina

(A, A', A'') Representative images of an adult wild type retina 4 weeks after the subretinal delivery of AAV2/8.CMV.hCLN6. Immunostaining reveals a widespread expression of *CLN6* in photoreceptors following subretinal administration.

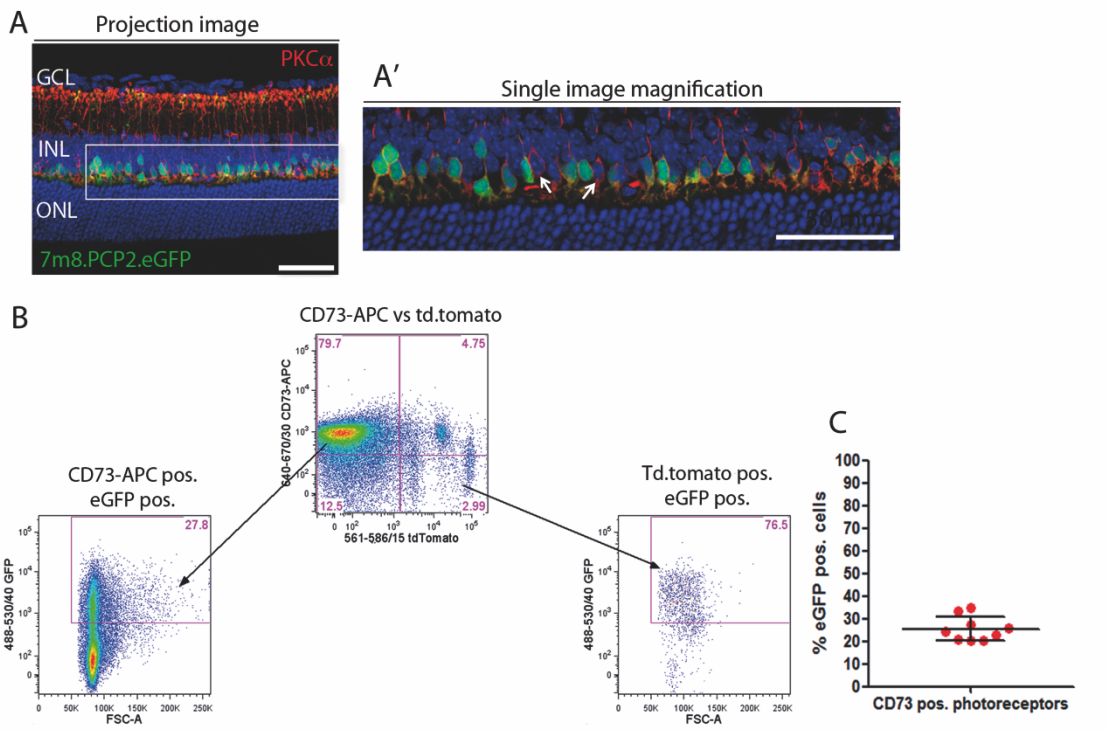

Figure S4: Transduction of retinal cell types after intravitreal injection of AAV serotype 7m8

(A, A') Representative images of wild type retinas 3 weeks after intravitreal administration of 7m8.PCP2.eGFP at P5. The majority of PKCα-positive cells expressed eGFP (arrows indicate rod bipolar cells not positive for eGFP). (B) Flow cytometry strategy to analyze the transduction efficiency of photoreceptors and bipolar cells in P5-P6 PCP2.Cre/td.tomato mice following the intravitreal delivery of 7m8.CMV.eGFP. Photoreceptor cells were labelled using the cell surface marker CD73 and bipolar cells were labelled with td.tomato in PCP2.Cre/td.tomato retinas. (C) Quantification of the photoreceptor transduction efficiency following 7m8 administration revealed that approximately 25 % of the CD73-positive cells were also positive for eGFP (mean ±SD), $n = 9$ eyes. Scale bars 50 µm.

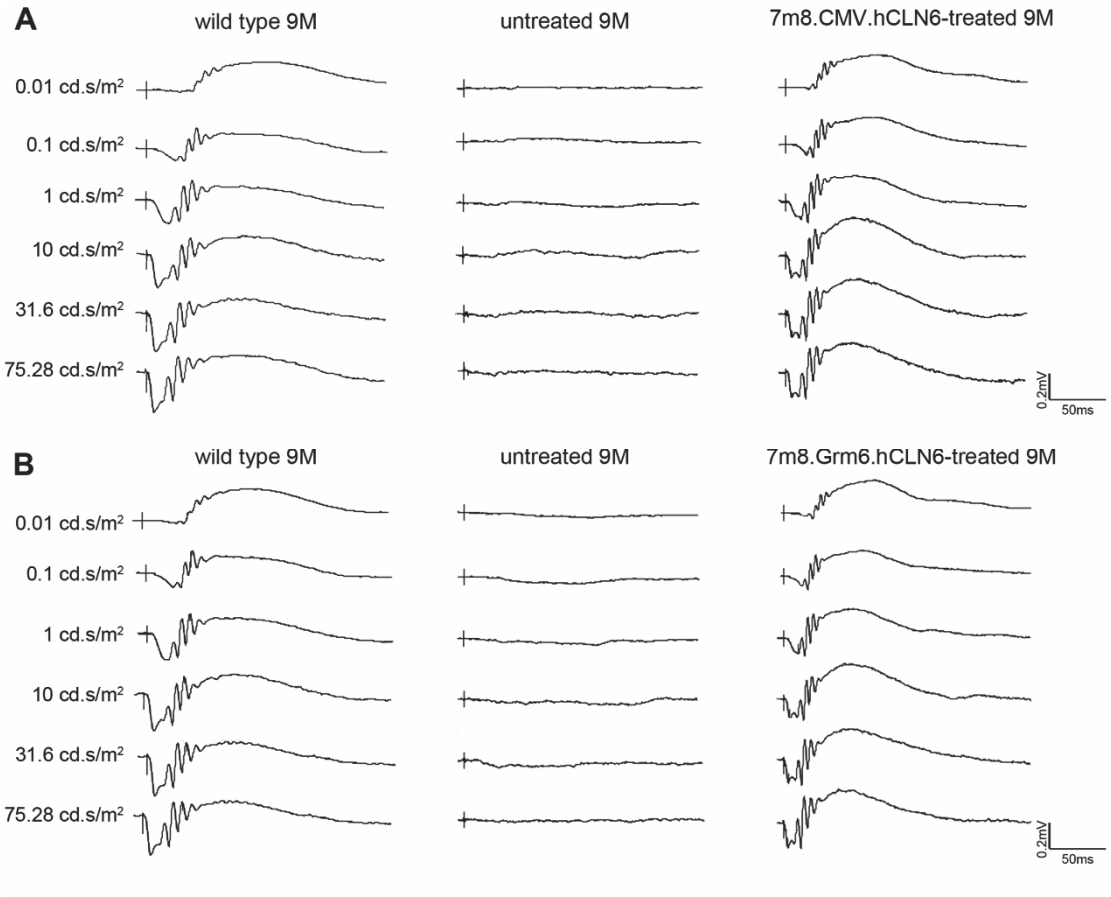

Figure S5: ERG raw traces

(A) Representative scotopic ERG raw traces from a wild type mouse at 9 months of age compared to an age-matched *Cln6*^{nclf} mouse that received intravitreal injections of 7m8.CMV.hCLN6 at a dose of 1x10^{9} vg in one eye. The contralateral eye was left uninjected. (B) Representative scotopic ERG raw traces from a wild type mouse at 9 months of age compared to an age-matched *Cln6*^{nclf} mouse that received intravitreal injections of 7m8.Grm6.hCLN6 at a dose of 1x10^{10} vg in one eye. The contralateral eye was left uninjected.